ELSEVIER

Biophysical Chemistry 85 (2000) 59–78

Biophysical Chemistry

www.elsevier.nl/locate/bpc

The positive role of voids in the plasma membrane in growth and energetics of *Escherichia coli*

S. Natesan, C.N. Madhavarao, V. Sitaramam*

Department of Biotechnology, University of Pune, Pune 411 007, India

Received 17 December 1999; received in revised form 13 March 2000; accepted 15 March 2000

Abstract

Bacterial respiration, endogenous as well as induced respiration by glucose, lactose and glycine betaine, was found to be sensitive to external solute concentration. Permeability of hydrogen peroxide, a non-electrolyte of molecular size between water and urea, through the bacterial membranes changed directly with the rate of respiration (an activity residing in the bacterial plasma membrane) in *E. coli* and the enhanced permeability and respiratory activity were highly correlated. Hydrogen peroxide permeability and induction of voids (spaces in the matrix of the bilayer into which hydrophobic fluorescent probes partition, which in turn were used to assess the modulation of these cavities) were shown to be a direct and excellent measure of leak conductance. Fluorescence intensity and anisotropy of the extrinsic fluorescent probes (incorporated by growing bacteria in their presence) decreased with increased respiration in bacteria, consistent with lowered molecular restriction and enhanced hydration in the membrane phase for these probes as seen in dimyristoylphosphatidylcholine bilayers due to phase transition. The physical basis of osmotic phenomena, as a relevant (thermodynamic) volume, could relate to water exchange or compression, depending on the osmotic domain. In the domain of compression in bacteria, i.e. well above the isotonic range, the computed activation volume was consistent with voids in the membrane. This study emphasises a major role of leak conductance in bacterial physiology and growth.

Keywords: Osmotic sensitivity; Peroxide permeation; Fluorescence anisotropy; Respiration; *Escherichia coli*

* Corresponding author. Tel.: +91-20-565-5179; fax: +91-20-565-5179.
E-mail address: sitaram@unipune.ernet.in (V. Sitaramam)

0301-4622/00/$ - see front matter
PII: S0301-4622(00)00145-9

1. Introduction

Voids can be defined as internal cavities or spaces, hydrated or otherwise, in the membranes made up of lipid bilayer and proteins and these voids have a critical role in the function and dynamics of the biopolymers [1]. Physical perturbations such as external solute concentration, temperature and pressure affect the dynamics and associated functions of these biopolymers. Oxidative phosphorylation in mitochondrial membranes and photophosphorylation in chloroplast membranes were shown to be sensitive to the external solute concentration. It was also shown that such sensitivity does not reside in any single complex but in the diffusivity of quinones through compressible voids between the acyl chains [2,3]. A comparison for voids can be drawn in the literature on proteins and in molecular dynamic studies [4–6] as the unoccupied spaces in the polymer assembly. An important development with regard to voids is the use of osmotic sensitivity of hydrogen peroxide permeation as a measure of voids in the membrane [7]. The similarities run deep between the bacterial plasma membrane and mitochondrial inner membrane. The osmotic sensitivity offers a unique probe to delve into these similarities. As in the case of mitochondria, bacterial energetics have made significant advances by way of explicit thermodynamic treatments, in spite of the complexities of the systems [8,9].

We have investigated the osmotic responses in *E. coli* from the point of view of energetics. It could be generalised that growth (energy dissipator) ceases well before respiration (energy source), in all aerobes thus far tested. The link with osmolality and growth itself is very interesting since one could identify a variety of osmotically responsive volumes in the physiology of an organism to account for the osmotic sensitivity. Besides water-flux dependent-volume specific for the isotonic range of external osmotic pressure, a variety of polymeric volumes could be considered relevant to account for the osmotic sensitivity of different processes. Voids that occur in biopolymers (e.g. membranes and proteins), by virtue of being compressible, exhibit different energy requirements which could be assessed by non-linear osmotic methodology as critical osmotic pressures. We report here that leak conductance (across the membrane through such voids) plays a major role in bacterial physiology based on the present experimental results.

1.1. Theoretical considerations

Understanding cause–effect relationships in osmotic responses in bacterial physiology could be difficult. It is necessary to define the osmotically relevant terms theoretically and experimentally in bacterial and analogous systems, before attempting to unravel these inter-relationships.

Consider a vesicle of volume:

$$V_{\text{vesicle}} = V_{\text{internal}} + V_{\text{membrane}} \tag{1}$$

where, V stands for volume and,

$$V_{\text{membrane}} = V_{\text{lipid}} + V_{\text{voids}} \tag{2}$$

In the face of osmotic gradients across this vesicle, V_{internal} would obey the relationship:

$$\Pi \Delta V = nRT \tag{3}$$

where, ΔV is the volume of water displaced, Π the osmotic pressure, n the internal solute content, R the gas constant and T the temperature in Kelvin.

The internal energy,

$$U_{\text{internal}} = C_v \cdot T \tag{4}$$

where, C_v is the specific heat capacity. Therefore,

$$\Pi \Delta V = nRU_{\text{internal}}/C_v \tag{5}$$

Thus, volume changes would occur in a quantitative range of energy wherein the energy terms are the product of the pressure and volume change due to water. This can be investigated in a variety of ways for volume changes directly measured using a particle size analyser during osmotic

swelling. Activation volume obtained from variation in equilibrium processes has units of cubic centimetres per mole (of water).

Two problems beset the investigators, since some definition is required on how the range of tonicities may be compared. The problem is compounded by the fact that the domain of actual volume change (directly measured by morphometry, electrical impedance or indirectly by light scatter, ordinary or dynamic laser light scatter) is quite small. In fact, many effects are seen in the domain of compaction and not directly due to bulk volume changes. Fig. 1a,b is a cartoon diagram showing the likely physical state of the bilayer under various conditions and the corresponding changes in the components of the vesicle volume. From Fig. 1 it is clear that what would matter is the osmotic range of the actual measurement. If the observed effect is seen as a monotonic relationship across a wide range of osmolalities, there is no advantage in restricting the analysis of such a phenomenon to a specific domain: only of hypo- or hypertonicities. If the phenomena are exclusively seen in a hypertonic domain, wherein volume changes due to net water gain/loss are negligible, we need to invoke other variables, depicting a different volume. This is embodied in Eq. (1) where, V_{membrane} could be invariant in the domain of primary volume response (hypotonicity) of the vesicle. On the other hand, in the domain of compaction, the V_{membrane} would change due to compaction and this would necessarily involve the intermolecular spaces/voids, which alone would be compressible and not the hard sphere molecules (V_{lipid}). Voids, unlike structural cavities, are primarily statistical and not simply structural and hence the choice of the dynamic term voids. Voids can also change in the hypotonic domain due to a change in the V_{internal} while, in the domain of compaction voids must change. Thus, if the measure of voids changes monotonically across isotonicity, correspondingly voids can be described in the entire range of osmolality from hypo- to hypertonicity. The likely consequence of compaction is the hindered mobility of the fluorescent probe and in terms of measured anisotropy it would increase. This was shown in DMPC LUVs for the fluorescent probe DPH (Fig. 1c).

The corresponding equation of state for the voids appears from the elastic constraints that define the polymeric behaviour such that, notionally,

$$U_{\text{total}} = (\Pi \Delta V C_v)/nR + U_{\text{elastic}} \quad (6)$$

The term U_{elastic} itself can be expanded to include all the relevant stresses and strains of the polymeric/membrane structures, their areas and the structural voids. Basically, the energy term being additive, can be seen only at higher pressures. Intuitively, higher pressures/energies would be required to occlude pores that admit smaller particles since a greater level of compaction would be required. An investigation into osmotic scale of activities would, therefore, be an adequate description of the energy requirements of a process.

2. Experimental procedures

2.1. Materials

IPTG, ONPG, glycine betaine, non-electrolytes/polyols, DMF, DMPC and the fluorescent probes ANS and DPH were from Sigma Chemical Co., USA. Other fluorescent probes 2-AS, 6-AS, 9-AS and 12-AS [where, *n*-AS is *n*-(9-anthroyloxy) stearic acid] were obtained from Molecular Probes Inc., USA. All other chemicals used were of analytical grade. Deionised and filtered water of tissue culture grade (Labconco) was used in all experiments.

2.2. Measurements in unwashed cells of E. coli during growth period

E. coli C90 cells were grown in minimal medium [1 mM KH_2PO_4, 1.5 mM $(NH_4)_2SO_4$, 0.08 mM $MgCl_2$ and 1.8 μM $FeSO_4$ with 40 mM sodium phosphate buffer (pH 7.2) and 0.2% (w/v) glucose] at 37°C in a shaker water bath [10]. Aliquots of cells were taken for the various measurements

at different periods of growth without washing the cells with buffer.

2.3. Preparation of washed E. coli cells

E. coli C90 and *E. coli* K-12 were grown aerobically in the minimal medium. Inoculation and harvesting of bacteria was carried out at the logarithmic phase routinely monitored by turbidimetry. Growth was monitored as $O.D._{520}$ and the number of cells was calculated from detailed standard curves. These were obtained by colony

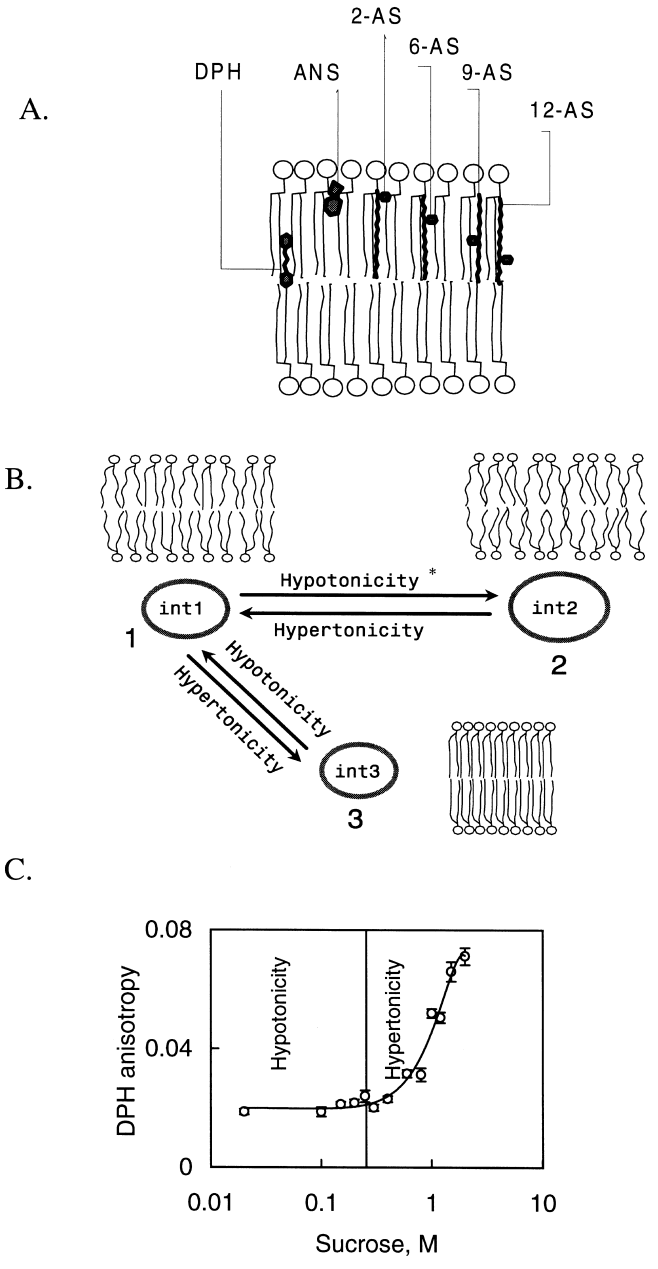

Fig. 1.

counts in plates after appropriate dilution and at least 2000 colonies were physically counted to minimise the counting errors at each dilution to prepare the $O.D._{520}$ vs. number of cells profiles. Cells were washed twice in 100 mM sodium phosphate buffer (pH 7.2; isotonic for the cells) at 4°C and centrifuged at $12\,000 \times g$ and these cells were maintained at 4°C for studies on respiration, hydrogen peroxide permeation and transport. The tonicity of the media was ascertained by a Wescor 5500 vapour pressure osmometer.

Bacteria were isolated from high salt as well as low salt and were washed also in high- and low-phosphate buffers and osmotic titrations of respiration were carried out. Basically, the profiles were consistent with accumulation of Na^+ in high-salt growth media, while the wash medium itself hardly affected the profiles in the range of 50–100 mM sodium phosphate buffer (data not shown).

2.4. Osmotic titration of swelling in bacteria

Bacterial cells (*E. coli* K-12, stock of 1.2×10^{11} cells) were suspended in different NaCl concentrations at 25°C in 1 ml of 10 mM Tris–HCl (pH 7.2) and the $O.D._{420}$ was monitored under constant stirring in a UV-vis spectrophotometer (Hitachi 220S). The cells exhibited invariably a decrease in $O.D._{420}$ except at very high osmolarities and/or molecular mass of the external osmolyte, consistent with swelling phenomena. The rate of decrease in $O.D._{420}$ was used as a measure of swelling in the bacterial cells [11]. The rate of swelling varied with external osmolarity permitting a detailed evaluation of the permeability to the external solute(s), which was highly comparable to mitochondria [12].

2.5. Measurements of respiratory rate in bacteria

Respiratory rates in washed bacterial cells were measured at 20°C in a medium containing different NaCl concentrations with 10 mM sodium phosphate buffer (pH 7.2), using a Clark-type oxygen electrode in a Gilson 5/6 Oxygraph. The oxygen electrode was calibrated by the standard method [13]. Specific activity was expressed as nanograms of atoms of oxygen consumed per minute per milligram of bacterial protein.

Protein concentration in the bacterial cells was estimated by using bovine serum albumin as the standard [14].

2.6. Transport of β-galactoside

The *Lac* operon was induced in the *E. coli* strains by growing the bacteria in minimal medium supplemented with 0.5 mM IPTG. The β-galactosidase activity was measured at 30°C in the presence of 5 mM ONPG as the chromogenic substrate [15], using a medium consisting of 2 mM Na_2HPO_4, 1.3 mM NaH_2PO_4, 0.33 mM KCl and 0.033 mM $MgSO_4$. Transport activity of lactose permease was monitored as the rate of *o*-nitrophenol formation, when the intact cells were incubated in the presence of ONPG. Specific activity was expressed as micromoles of ONPG

Fig. 1. Cartoon diagram of the most plausible position of fluorescent probes (heavy lines) in the lipid bilayer (A), the consequence of osmotic pressure on the volume of a bilayer vesicle and the physical status of the bilayer in steady-state condition (B), and the experimental data of DPH anisotropy in DMPC large unilamellar vesicles as a function of increasing tonicity in the external medium (C). (A) The probes are represented in only one-half of the bilayer though both halves are equally likely to harbour the probes. (B) Only relative volumes are represented. The numbers 1, 2 and 3 represent isotonicity, hypotonicity and hypertonicity of the external medium in which the vesicles are suspended and 'int' stands for the corresponding internal volume. The (*) indicates that the state '2' can be achieved by either hypotonicity of the external medium or by induction of respiration by substrates in organisms like *E. coli*. (C) External sucrose concentration is plotted on a log scale to specifically show the effect on 'hypo' and 'hyper'tonic domains and the vertical line represents the isotonicity [entrapped solution contained 200 mM sucrose, 10 mM NaCl and 10 mM sodium phosphate buffer (pH 7.4)]. Fluorescence anisotropy of the probes would increase in '3' as compared to '1' or '2', whereas it may decrease in '2' as compared to '1' owing to corresponding change in V_{void} in the membrane phase. From Eqs. (1) and (2) we can deduce the following such that, at steady state: (i) $V_{vesicle2} > V_{vesicle1} > V_{vesicle3}$; (ii) $V_{internal2} > V_{internal1} \geq V_{internal3}$; (iii) $V_{membrane2} \geq V_{membrane1} \gg V_{membrane3}$; and (iv) $V_{void2} \geq V_{void1} \gg V_{void3}$.

hydrolysed per minute per milligram of bacterial protein (millimolar extinction coefficient of ONPG at 420 nm = 3.22 at pH 7.2).

2.7. Measurements of hydrogen peroxide permeation

Occluded catalase activity [16] was assayed using a HP8450A diode-array spectrophotometer as the disappearance of H_2O_2 at 240 nm at 20°C [17]. The media consisted of different NaCl concentrations in 10 mM sodium phosphate buffer (pH 7.2) and 12 mM H_2O_2 with constant stirring and aeration. Specific activity was expressed as micromoles of H_2O_2 consumed per minute per milligram of bacterial protein. An aliquot of cells disrupted by a brief sonication on an ice-water bath was the source for total catalase activity, which was monitored during the entire growth period. Catalase activity was also measured polarographically as the evolution of oxygen upon addition of hydrogen peroxide [18] and expressed as nanograms of atoms of oxygen evolved per minute per milligram of bacterial protein.

2.8. Osmotic responses of E. coli growth in the presence of glycine betaine

Glycine betaine (0.5 mM) was prepared in 10 mM sodium phosphate buffer (pH 7.2). Bacteria in the presence and absence of glycine betaine were grown aerobically at 37°C in a shaker water bath at varying concentrations of NaCl. When the bacteria reached the logarithmic phase, an aliquot of 1 ml was taken from the cultures and the growth was monitored as $O.D._{520}$. The $O.D._{520}$ was converted to number of cells using the relationship $Y = 1.6 \times 10^{11} X + (-6.6 \times 10^{8})$, where, Y is the cell number and X is the $O.D._{520}$, which was determined empirically. Growth in the presence and absence of glycine betaine in *E. coli* was compared by plotting the number of cells as a function of the NaCl media. Cells were pre-incubated for 5 min in different NaCl media in the absence and presence of glycine betaine along with 10 mM glucose.

2.9. Osmoprotective role of glycine betaine vis-à-vis various substrates in the growth of E. coli MC 4100

Bacteria were grown with glycerol, glucose, mannitol and trehalose as the substrates at 10 mM, each as an exclusive carbon source in a minimal medium. The $O.D._{520}$ of media at a time corresponding to the logarithmic phase of control cells was plotted as a function of the NaCl concentration. The critical NaCl concentration at which growth ceases was obtained for each substrate in the presence and absence of 0.5 mM glycine betaine. The data were obtained in a single experiment with all the substrates for approximately 12–18 concentrations of NaCl for each substrate. Organic acids, pyruvate, lactate and succinate (10 mM each) were also used as substrates in a parallel experiment.

2.10. Preparation of DMPC vesicles

Large unilamellar vesicles (LUVs) were prepared by reverse phase evaporation by incorporating an aqueous solution consisting of 200 mM sucrose, 10 mM NaCl and 10 mM sodium phosphate buffer (pH 7.4) [19] and resuspended in isotonic ($\sim$ 280 mOs/kg) sucrose medium. DPH was incorporated by incubating aliquots of vesicle ($\sim$ 0.5 mg/ml) with 12.5 μM DPH (final concentration), in dark for 30 min and were used for measurement of DPH anisotropy as a function of sucrose concentration. Vesicles were maintained at 30°C throughout, i.e. above phase transition temperature of DMPC ($\sim$ 24°C). Multilamellar vesicles (MLVs) were prepared [19] and resuspended into a medium of 0.155 M NaCl in 10 mM sodium phosphate buffer (pH 7.2). Small unilamellar vesicles (SUVs) were prepared by sonicating the MLVs in a probe-type sonicator (Branson) into a clear suspension and pelleted by centrifuging at $200\,000 \times g$ for 1 h at 25°C and re-suspended in the same medium. These SUVs were used for phase transition measurements with all the fluorescent probes.

2.11. Phase transition measurements with fluorescent probes

The relative changes in the fluorescence intensity of an incorporated fluorophore can be a measure of thermal transitions in lipids [20]. Fluorescence intensity and anisotropy of the incorporated probe was monitored using a Kontron SFM25 spectrofluorometer. Temperature transition of DMPC SUV's was measured with the incorporated fluorophore, while heating the sample in the cuvette at the rate of 0.5°C/min using a Haake circulating water bath and Haake F3 thermoregulator controlled by a PG 20 programmer. Fluorescence anisotropy (r) was calculated from fluorescence polarisation, P [20] as follows:

$$P = (I_{vv} - G \cdot I_{vh})/(I_{vv} + G \cdot I_{vh}) \quad \text{where}$$
$$G = (I_{hh}/I_{hv}) \tag{7}$$

$$r = (2P)/(3 - P)$$

where, I is the fluorescence intensity, v and h stand for the polariser placed vertically and horizontally, respectively, and the double subscripts stand for the excitation and emission polarisers. The correction factor G was calculated at every polarisation value using the horizontally polarised light (i.e. for each polarisation value, a set of four fluorescence measurements were used with the excitation and emission polarisers oriented in all four combinations). In all measurements reported here, the G-value was seen to be close to 1.0 (range 1.0–1.25) thereby ensuring that the emission monochromator did not contribute significantly to polarisation effects at the wavelengths used. The temperature in the cuvette was independently monitored using a temperature probe connected to a Hewlett Packard 89100A temperature controller and recorded on a Hewlett Packard 85B microprocessor. Continuous on-line measurements of fluorescence were made on a Kontron SFM25 spectrofluorometer and accumulated every 12 s onto an IBM compatible 286 PC. In all the phase transition measurements the probe-to-lipid ratio was 1:200.

2.12. Fluorescence intensity and anisotropy measurements in E. coli

The fluorescent dyes ANS, DPH and the n-AS depth probes were prepared in distilled water, dimethyl formamide and ethanol, respectively. Probes dissolved in distilled water were filter-sterilised using 0.45-μm HWAP Millipore filters and those dissolved in organic solvents were filtered using 0.45-μm FHLP Millipore filters. A fluorescent dye dissolved in organic solvent, after filter sterilisation, was smeared on the bottom and sides of sterile culture flasks by evaporating the solvent, into which the sterile aqueous growth medium was added and used for bacterial growth. The cells were harvested at the logarithmic phase by centrifuging at $12\,000 \times g$ at 4°C and washed twice with 100 mM sodium phosphate buffer (pH 7.2). The fluorescence measurements were carried out at 20°C with constant stirring and aeration, in a Kontron SFM25 spectrofluorometer.

Polarization measurements were made in the automated mode as described above. Approximately 30 polarisation readings were made at 12-s intervals before and after addition of glucose and only the mean values were used for representation.

Approximately 7.2×10^{10} bacterial cells with incorporated fluorophores were suspended in media containing 0.155 M NaCl in 10 mM sodium phosphate buffer (pH 7.2) and aerated by bubbling air during the measurements at 20°C. Fluorescence anisotropy was continuously monitored at 12-s intervals in the automated mode as described above. After 5 min, 10 mM glucose was injected into the reaction mixture and recording was continued for another 5 min. As controls, the oxygen content was depleted by bubbling nitrogen into the medium during the assay.

The amount of fluorescent probe incorporated into the bacterial cell membrane was determined by extracting the probe in a chloroform:methanol mixture (2:1, v/v) and measuring the fluorescence intensity in ethanol. Uncorrected excitation and emission spectra were obtained for all probes for comparison. Excitation and emission wavelengths for the different probes were: ANS, 360 and 450 nm; DPH, 355 and 430 nm; and for the n-AS

probes, 360 and 460 nm, respectively. The amount of fluorophore was estimated from standard curves of fluorophore concentration vs. relative fluorescence intensity in ethanol.

2.13. Measurement of critical pressures for cessation of osmotically sensitive activities: break-point analysis

Osmotic responses have been shown to be segmentally linear in a variety of situations. The limits of linear responses could be readily obtained by spline regression techniques. The variance associated with the break-point (the projection of discontinuity onto the abscissa, osmotic pressure) was solved using a boot-strap technique based on Hudson's algorithm with the help of a computer programme to assess the discontinuities [21]. The significant osmotic response considered here was one of inhibition, resulting in a discontinuity (i.e. break-point) beyond which osmotic response was marginal. For this reason the spline regression in the hypotonic domain was omitted due to plurality of causes. The computer programme essentially determines iteratively a two-spline regression such that the unaccounted variance by this procedure is far less compared to single regression for all the data points. Typically the analysis in all reported data was such that the NRSS (the unaccounted variance as a fraction of total variance) was less than 5%. The break-point concentration of the external osmolality carries specific information for an osmotically sensitive process, i.e. the critical pressure at which a particular process ceases. The larger the break-point the larger the energy required to stop a process, i.e., to compress a relevant volume. In the figures showing break-points isotonicity is indicated by vertical lines.

2.14. Measurement of activation volume of processes

It is possible to define a relevant volume (activation volume) in an energy-related scale which is inversely related to the critical pressure (break-points). The activation volume was calculated using the relationship:

$$\Delta V = -RT \ln J_{rel}/\mathrm{d}P \quad (8)$$

and

$$J_{rel} = J_{osm}/J_o$$

where, J_{rel} is the relative activity, J_{osm} is the activity at a given osmolarity, J_o is the lowest activity measured in that range, R is the gas constant, T is the absolute temperature, P is the osmotic pressure (where, $P = cRT$ and c is the molarity of the external osmolyte) and ΔV is the activation volume [22]. Since the relationship need not be linear in the logarithmic scale of relative activity as a function of osmotic pressure (in atmospheres), it was convenient to determine the maximal negative slope with the best possible fit iteratively. In all instances, the data uniformly represented the best-fit maximal negative slope. Three criteria were chosen for comparison among activation volumes: (i) overlapping ranges of pressure; (ii) activation volume for the effects (energy dissipators) would be equal to or more than causes (energy generators); and (iii) the critical pressures (break-point) are inversely related to activation volume. Hence, it was not considered to be necessary to compute the activation volume using the same range of pressures, nor is it practical.

3. Results and discussion

3.1. Effect of external solute concentrations on basic microbial energetics

Fig. 2 shows the plots of specific activities, (namely, swelling, respiration, growth and transport) vs. the external NaCl concentration. The comparisons were made based on the reasonable premise that these *E. coli* have isotonicity at ~ 300 mOsm/kg [23].

3.2. (i) Turbidimetric measurements of bacterial swelling

E. coli shares the non-adiabatic behaviour of mitochondria [24] in that, while the external NaCl behaves as an osmolyte in inducing volume

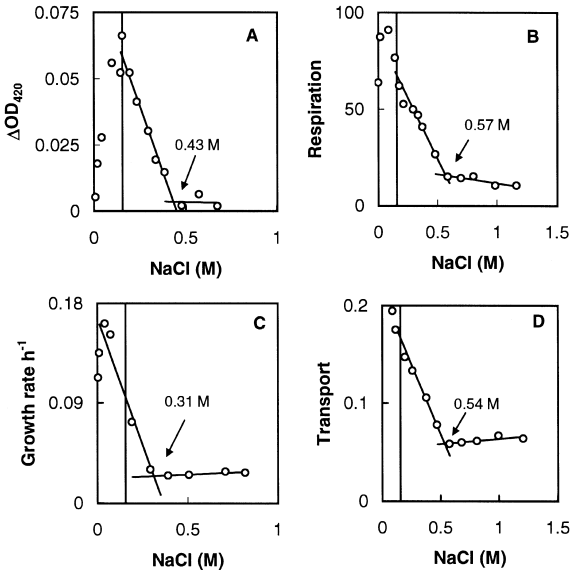

Fig. 2. Effect of external NaCl media on various physiological processes in *E. coli* K-12. Turbidimetric changes (= swelling) (0.43 M, 2767 cm^3/mol) was measured as rate of change of $O.D._{420}$ (A). Endogenous respiration (0.57 M, 1363 cm^3/mol) was measured polarographically as nanograms of atoms oxygen consumed per minute per milligram of bacterial protein (B). Growth rate (0.31 M, 3164 cm^3/mol) was measured as rate of change of $O.D._{520}$ (C) and transport of β-galactoside (0.54 M, 1275 cm^3/mol) was measured as micromoles ONPG hydrolysed per minute per milligram of bacterial protein (D). The values in parentheses indicate the break-point and the activation volume, respectively.

changes, the bacterium exhibits volume changes even in isotonic NaCl media. This non-adiabatic behaviour can be explained only if the bacterial membranes exhibit permeability to the external solute NaCl. In the case of mitochondria, respiration was shown to induce voids in the inner membrane and thereby enhance permeability to external solutes [24]. This spontaneous swelling of mitochondria is considerably different from (and should not be confused with other modes of swelling) calcium-induced swelling due to the mitochondrial permeability transition pore in the inner membrane [25]. This spontaneous swelling represents an induced porosity inherent to mitochondrial respiration (seen with oxidative phosphorylation) as low amplitude swelling. In case of other eukaryotic cells, another class of phenomena due to specific channels come under the category of regulatory volume increase, RVI, and regulatory volume decrease, RVD [26], and the latter was not observed during mitochondrial swelling [24]. Fig. 2a shows that *E. coli* exhibits a swelling response, the rate of which was inhibited by increasing the NaCl concentration in the media. The osmotic susceptibility of this swelling was seen to reflect an activation volume of 2767 cm^3/mol. One would need to determine if this swelling required respiration.

3.3. (ii) Osmotic sensitivity of bacterial respiration

Endogenous as well as exogenous respiration in mitochondria was shown to be sensitive to external osmotic pressure. Bacterial electron transport is also quinone dependent [27] similar to mitochondria and chloroplasts [2] and an osmotic inhibition was seen with an activation volume of 1363 cm^3/mol for endogenous respiration as shown in Fig. 2b. Endogenous respiration was used to assess the osmotic sensitivity to avoid the requirement for substrate transport, which may have a confounding effect. Respiration being the source of energy, showed two times less osmotic sensitivity compared to the swelling phenomenon. The break-points showed an inverse relation with the activation volume as can be discerned from Fig. 2a,b. This indicates that parameters other than respiration, significantly contribute to the swelling phenomenon.

3.4. (iii) Osmotic sensitivity of growth rate

The effect of external solute concentration on growth rate of *E. coli* is shown in Fig. 2c which shows the activation volume of growth to be 3164 cm^3/mol, indicating higher sensitivity than the endogenous respiration (2.3-fold), but similar to swelling phenomenon (1.1-fold). The critical pressure at which growth was inhibited was considerably less compared to respiration. This is consistent since growth also involves, in addition to endogenous respiration, uptake of external substrates, so there could be several intervening steps including transport which would be osmotically sensitive.

3.5. (iv) Osmotic sensitivity of transport

Transport of β-galactosides could be readily assessed in *E. coli* in which the *lac* operon is induced by using the chromogenic substrate assay with ONPG. Transport shown in Fig. 2d indicates: (i) the activation volume of the β-galactoside transport was 1275 cm^3/mol, which was indistinguishable from that of respiration; (ii) transport was inhibited on addition of uncouplers under aerobic [28] as well as anaerobic conditions [29]; (iii) V_{max} alone was affected and not the K_m ; and lastly, (iv) the stoichiometry of β-galactoside transported to oxygen consumed remained invariant in the osmotically sensitive domain of transport under identical assay conditions (data not given). Thus, the active transport of β-galactoside was related to bacterial respiration with respect to external osmolality as judged by the activation volumes as well. It is irrelevant whether respiration is coupled to lactose transport directly or via protonmotive force, since the components of the coupled system are equally sensitive to osmotic pressure as evidenced by a constant stoichiometry. The enhanced sensitivity of growth and swelling require additional variables sensitive to external solute concentration that need to be identified.

In order to understand osmotic sensitivity in the relevant range above isotonicity, it is essential to measure compaction by a variety of membrane probes.

3.6. Hydrogen peroxide permeation as a probe for voids in the membrane

Hydrogen peroxide permeation across membranes exhibited marked osmotic sensitivity in several cells (including *E. coli* inner membrane) and organelles, and this was traced to the lipid composition per se. The only exception was erythrocytes; the cells as well as the liposomes made from the lipids of these cell membranes exhibited a lack of osmotic sensitivity and this was traced to the void annealing effect of cholesterol esters richly present in these membranes [7]. Peroxide permeation itself was readily measurable with adequate care taken to ensure absence of peroxidative damage to membranes [7]. Under initial velocity conditions, the rate of peroxide permeation would be equal to the rate of degradation of the permeated peroxide by the occluded catalase. Kinetics would be more complex for the activity since the occluded enzyme would require correction for the efficiency parameter for the unstirred layers within the vesicle. Fig. 3 shows the osmotic sensitivity of the peroxide permeation in *E. coli* cells (Fig. 3a) and liposomes made from the lipids of these bacterial membranes (Fig. 3b), with activation volumes corresponding to 340 and 1364 cm^3/mol, respectively. The annealing effect of protein appears to be similar to that of sterols in decreasing the osmotic susceptibility of lipid bilayers and the peroxide permeation. In all these studies, the total catalase activity was monitored in cells disrupted by sonication and any significant inactivation of the internal catalase was ruled out experimentally (data not shown).

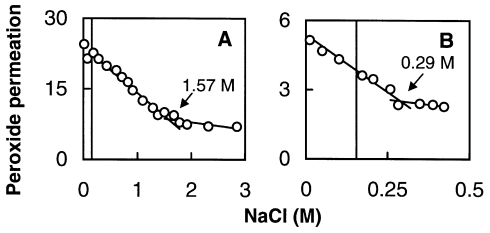

Fig. 3. Critical osmolarities for hydrogen peroxide permeation in *E. coli* K-12 cells (A) and liposomes made of lipids extracted from the bacterial cells (B). The activation volume for the bacterial cell was 340 cm^3/mol and for liposomes 1364 cm^3/mol.

3.7. Is stimulation of respiratory rate coupled to the rate of peroxide permeation?

Respiration in *E. coli* increases in the presence of exogenous glucose. The effect of respiration on peroxide permeation can be assessed by following the rate of respiration and peroxide permeation in the absence and presence of glucose. Fig. 4a,b shows the plots of endogenous and glucose-induced respiration, respectively, measured as a function of NaCl concentration. Most notable was the observation that the activation volume of respiration enhanced from 1676 to 2424 cm^3/mol

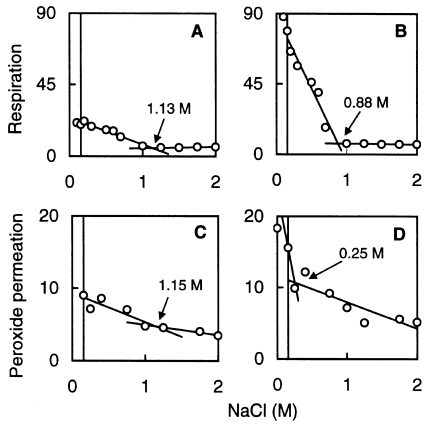

Fig. 4. Effect of external NaCl concentration on respiration and hydrogen peroxide permeation in *E. coli* C90. Respiration is shown as nanograms of atoms oxygen consumed per minute per milligram of bacterial protein and with break-points of 1.13 M in the absence of glucose (A) and 0.88 M in the presence of 10 mM glucose (B). Peroxide permeation is depicted as micromoles H_2O_2 consumed per minute per milligram of bacterial protein and with break-points of 1.15 M in the absence of glucose (C) and 0.25 M in the presence of 10 mM glucose (D). The activation volumes obtained were 1676 and 2424 cm^3/mol for respiration in the absence and presence of glucose, respectively; similarly, 293 and 536 cm^3/mol for peroxide permeation.

in the presence of glucose, showing ~1.5-fold enhanced osmotic sensitivity. Peroxide permeation under identical experimental conditions was monitored as shown in Fig. 4c,d, and this closely reflected the changes similar to respiration. The activation volume increased from 293 to 5536 cm^3/mol in the presence of glucose. An inverse correlation could be readily observed between the activation volume and the break-point in each of these experiments. These provided the following information: (i) peroxide permeation and respiration were directly related; (ii) while respiration could be inhibited nearly completely, peroxide permeation was finite; (iii) this threshold increased in the presence of glucose; and (iv) on addition of glucose, peroxide permeation was enhanced. The osmotic pressure required to inhibit respiration was less than that required to inhibit hydrogen peroxide permeation. It stands to reason that a larger void (required for quinone) collapses much more readily than a smaller one (required for H_2O_2) under a given osmotic compression (similar to energy of polar contacts in cavities in proteins, which reduces with the increasing number of contacts, i.e. size of cavity; [30]). The stimulation of peroxide permeation by glucose could not be explained by its stimulation of respiration alone.

In bacterial cells kept under anaerobic conditions (by bubbling nitrogen), the changes in peroxide permeation were not observed on addition of glucose (data not given). Thus, active respiration was a necessary component for enhanced peroxide permeation. The subsequent utilisation of the sugar was not required for stimulation of respiration and thus it was fruitfully compared to respiratory control. Non-hydrolysable sugars were also shown to stimulate respiration [31]. Enhanced non-ohmic conductance due to respiration even in mitochondria remains an oddity, since leakiness of the membrane to a variety of solutes has not been assessed [32]. The induction of voids by glucose due to its transport would critically account for stimulation of respiration, since the presence of large enough voids would enhance the quinone mobility. Such pores would readily admit hydrogen peroxide, which is much smaller. However, as a consequence of their size differences, the larger pores that admit the quinone would be far more readily compressed than the fine pores that admit the peroxide alone, as seen above. Thus, the differential osmotic threshold for inhibition would be an expected consequence of different molecular sizes of the relevant diffusive species for respiration and peroxide permeation.

3.8. Calibration of fluorescent probes in membranes

Induction of respiration in bacteria by exogenous glucose is nearly instantaneous. Thus, any changes in the membrane that are causal to this induction would also be instantaneous. We, therefore, used a series of surface and depth fluorescence probes to assess the changes in fluorescence intensity and fluorescence anisotropy, initially in liposomes as a model membrane system, for further comparison with the bacterial membranes. It was convenient to use DMPC which exhibits an excellent phase transition at ~24°C

[33,34] which is associated with drastic change in the ordered bilayer. This would provide unambiguous changes in fluorescence intensity and anisotropy of the probes as a consequence of changes in voids of the bilayer.

The first derivatives of the polynomial best-fits at the transition temperature (T_c) gave information as to which probe had the maximal change in tumbling, i.e. anisotropy, and which had experienced maximal change in hydration in the microenvironment, i.e. fluorescence intensity, shown in Fig. 5a,b. We have examined the fluorescence lifetime of DPH in DMPC vesicles under frozen (gel) and liquid–crystalline (sol) conditions of DMPC. Under these conditions the fluorescence intensity as well as fluorescence anisotropy showed a marked decrease on melting, as did the mean lifetime of DPH (9.07 ns in gel–7.38 ns in sol condition). This large change in DPH lifetime was consistent with induction of voids (changes in molecular restriction parameter). The faster decay in DPH fluorescence intensity is characteristic of enhanced hydration (data not given). The *n*-AS probes exhibited parallel changes to that of DPH, both in anisotropy and fluorescence intensity, offered a similar interpretation. ANS on the other hand, showed an increase in fluorescence intensity, while the anisotropy decreased at phase transition.

Fig. 5a,b shows the extent of change for each of the probes in fluorescence anisotropy as well as fluorescence intensity during phase transition. The liposomal membranes were best evaluated by DPH, a routinely used probe for membrane studies. These measurements were extended to bacteria and were assessed independently for the

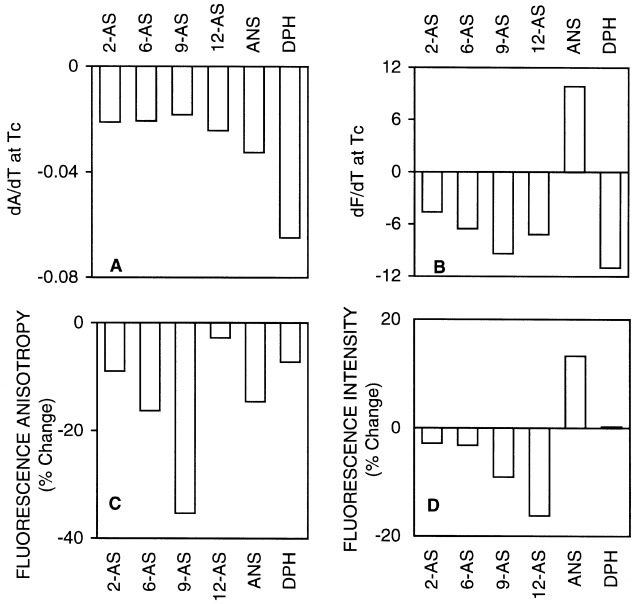

Fig. 5. Transition-induced changes in the lipid bilayer as reported by various fluorescent probes in DMPC vesicles. First derivative values of anisotropy (A) and fluorescence intensity (B) at transition temperature (T_c) for the *n*-(9-AS) series of probes, ANS and DPH. These values were obtained from the first derivative of the temperature vs. anisotropy and temperature vs. fluorescence intensity plots, respectively, after fitting the curve to a polynomial of adequately high order such that $r \geq 0.99$. Glucose induced changes in the fluorescence anisotropy (C) and intensity (D) of various probes incorporated in cells of *E. coli* C90 during growth. Percentage change is expressed as: $[I_{(+\text{glucose})}] - [I_{(-\text{glucose})}]/[I_{(-\text{glucose})}] \times 100$, where, $I_{(+\text{glucose})}$ is the fluorescence intensity or anisotropy value after addition of glucose and $I_{(-\text{glucose})}$ is the value before addition of glucose. The fluorescence intensity and anisotropy values are mean values of 30 readings. Means were compared using Student's *t*-test. All probes showed significant changes in both fluorescence intensity and anisotropy but for DPH, for fluorescence intensity. Typically, the coefficient of variation in these data was $\leq 1\%$ ($n = 30$).

changes on addition of glucose. The depth probes did not show the same rank order of signal in bacteria as in liposomes (Fig. 5c,d). 12-AS showed large fluorescence intensity in bacterial membranes though not in fluorescence anisotropy, while 2-AS showed the least fluorescence intensity. DPH did not serve as a useful probe in bacterial membranes, in these studies. The results suggested that the orientation and penetration by these probes could be influenced by the presence of protein so as to differ to some extent in the responses from the liposomal membranes. On addition of glucose, the fluorescence intensity decreased in bacteria for each of the probes except for ANS which showed an increase: (i) the change in fluorescence intensity was rapid in time though small, but significant in magnitude for the *n*-AS probes; (ii) the magnitude of changes observed was much larger than that due to dilution alone and was highly reproducible; and (iii) there was no spectral shifts in the uncorrected emission scans. No changes in fluorescence intensity and fluorescence anisotropy were seen under anaerobic conditions [35].

These studies helped to ascertain the induction of voids in the bacterial plasma membrane by comparing the effects with a known phenomenon in a known system as in phase transition in pure lipid bilayer. Fig. 6a shows the effect of phase transition in DMPC vesicles, while Fig. 6b shows the effect of glucose on the *E. coli* membrane with various probes in a plot of fluorescence intensity vs. anisotropy. While fluorescence intensity would be in arbitrary units and not necessarily comparable, particularly from probe to probe, anisotropy in the observed units match with the expectations depending on the locus of the probe (see Fig. 1a). For instance, the peripheral 2-AS would exhibit a greater anisotropy than the more interiorly located 12-AS. It is particularly noticeable that phase transition has led to a decrease in the anisotropy as well as fluorescence intensity. A decrease in anisotropy would be best interpreted as a decrease in the molecular restriction parameter [36] due to induction of voids/defects in the bilayer during phase transition and after melting into the sol state, and is well documented in the literature [37,38]. The decrease in fluorescence intensity was seen uniformly with all the probes, and for DPH, it is well documented to be due to an increase in hydration [20,39,40].

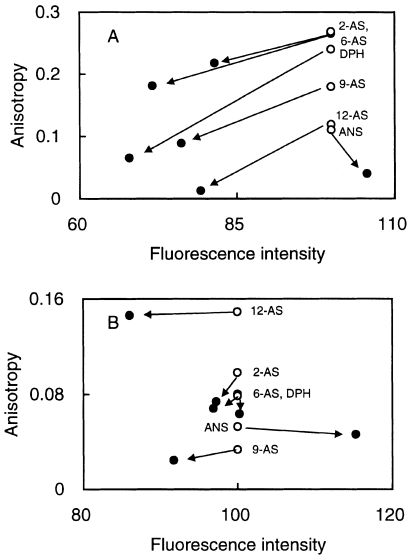

Fig. 6. Fluorescence intensity vs. anisotropy plots of various probes incorporated into DMPC SUV (A) and *E. coli* C90 cells (B). Fluorescence intensity and anisotropy values in (A) represent mean values of 10 readings at gel condition (o—o, 21°C) of DMPC normalised to 100 on the fluorescence scale and at sol condition (●—●, 28°C) of DMPC not normalised, specifically to show the direction of change when voids are induced in the bilayer, after lipid phase transition. Similarly, values in (B) represent mean values of 30 readings before addition of glucose (o—o) normalised to 100 on the fluorescence scale and after addition of glucose (●—●) not normalised, to show the direction of change which was similar to that of the gel–sol transition in DMPC bilayer.

ANS and the *n*-AS probes yielded similar results in bacterial membranes due to perturbations and the induction of respiration due to glucose that were comparable with the phase transition response in DMPC SUV (see Figs. 5 and 6).

In order to ascertain where the probes get incorporated, and, the extent of incorporation in each of the two membranes of the bacterial cell, we prepared spheroplasts [41] from the fluorophore-incorporated cells. As a control, spheroplasts were prepared from the cells without the probe. Fig. 7 shows the uncorrected emission spectra of 9-AS in the bacterial cells and the respective spheroplasts prepared from those cells.

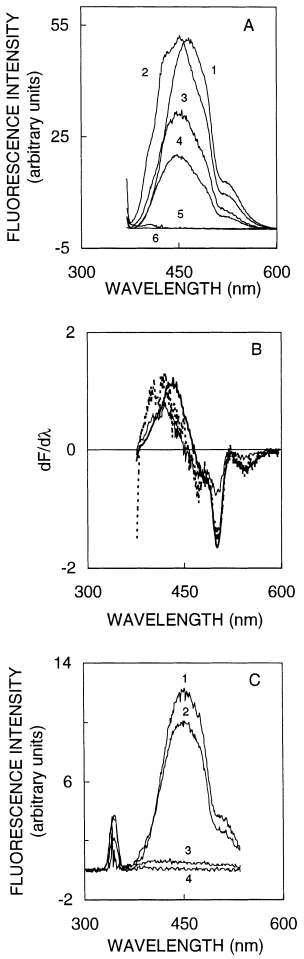

Fig. 7. Fluorescence emission spectra of 9-(9-AS). The uncorrected emission spectra of 9-AS (A) in: ethanol (1); *E. coli* C90 (2); DMPC SUV (3); supernatant of the bacterial culture (4); phosphate buffered saline (5); and DMPC SUV without the probe (6). The first derivative of 9-AS uncorrected emission spectra (B) in ethanol (—), in *E. coli* C90 (...) and in DMPC SUV (—). Values represent moving average over 9 nm ($n = 4$). Note a small but consistent blue shift in the peak fluorescence of 9-AS in the bilayer as compared to the one in ethanol. Uncorrected fluorescence emission spectra of 9-AS in *E. coli* C90 (C) in: cells (1); spheroplasts (2); spheroplasts incubated with 9-AS for 1 h (3); and spheroplasts without 9-AS (4).

More than 80% of the fluorescence signal was found in the spheroplast itself indicating that there was a maximal incorporation of the probe in the plasma membrane. The extent of incorporation of the *n*-AS probes was: 2-AS, 12.7% (w/v); 6-AS, 7.2% (w/v); 9-AS, 8.9% (w/v); and 12-AS, 10.2% (w/v) of the initial amount of 190 μg probe/cm^3 used. Since it would be difficult to assess the exact probe:lipid ratios in growing bacteria, the bacteria were grown in varying amounts of the probe (1–4 μg/cm^3 in the medium) and ascertained that the fluorescence intensity response was linear in this range as judged by the signal obtained. The probe concentration was chosen well within this linear range of fluorescence intensity response at a given bacterial density, which would be consistent with low, if any, interference due to inner filter effects.

When the control spheroplasts (those without probe) were incubated with 9-AS for 1 h, very little fluorescence intensity was observed, indicating very poor incorporation of the probe. This further confirmed that the fluorescent probes can be incorporated efficiently only during the growth phase of the bacteria.

These observed changes in fluorescence intensity and anisotropy (Figs. 5 and 6) would be consistent with an increase in permeation of water and other non-electrolytes. If glucose-induced osmotically compressible voids in the membrane forms the basis of the observed fluorescence intensity and anisotropy changes, it would be logical to conclude that there could be a general mechanism for ligand-mediated enhanced leak conductance in bacteria. The molecule of interest for this class of effects was glycine betaine, a well known osmoprotectant in *Enterobacteriaceae* [42–44].

3.9. Effect of glycine betaine on growth, respiration and peroxide permeation

Fig. 8a,b shows the effect of glycine betaine on the growth of *E. coli* C90. The activation volume increased from 4324 ± 162 to 5428 ± 360 cm^3/mol ($n = 4$) and the increase was shown to be significant ($P \leq 0.01$) by the Student's *t*-test. The break-points were also significantly different ($P \leq 0.01$) as tested by Student's *t*-test in multiplicates ($n = 4$) as well as by the automated procedure based on Hudson's algorithm [22]. Since external solutes like glycine betaine, choline, proline, and glucosylglycerol can accumulate inside het-

erotrophic eubacteria and cyanobacteria [29,42,44–47], we evaluated the effect of glycine betaine on respiration (shown in Fig. 8c,d) in cells grown in 0.3 M NaCl. Glycine betaine stimulated respiration further, changing the activation volume by ~threefold (1656–4905 cm^3/mol). The break-points and activation volumes were found to be significantly different ($P \leq 0.01$) by both Student's *t*-test as well as by the boot-strap methodology. Thus, the mechanism of action of glycine betaine should be comparable to that of glucose which was consistent with induction of voids in the bilayer. This could be tested directly. If glycine betaine stimulates respiration and induces voids, the mechanism of osmoprotection offered by glycine betaine could also be due to enhanced leak conductance to the substrate. If so, there should be some relationship between the molecular mass of the substrate for growth and osmotolerance. While the strains of *E. coli*, K-12 and C90 exhibited a larger tolerance for NaCl, MC4100 exhibited marked sensitivity such that the salt inhibited growth at < 0.4 M (data not shown). Under these conditions, various polyols were used as substrates for growth, and the results are summarised in Table 1. The data show that there was a marked difference in the osmotolerance conferred by glycine betaine in the presence of polyols. In the case of organic acids there was hardly any difference in the conferred osmotolerance by glycine betaine (data not shown). The limiting osmolarity was directly related to the molecular size of the substrate molecules, e.g. the bacteria grew in up to 0.9 M NaCl medium in glycerol (92 Da) as compared to 0.4 M NaCl in trehalose (342 Da), [29,48].

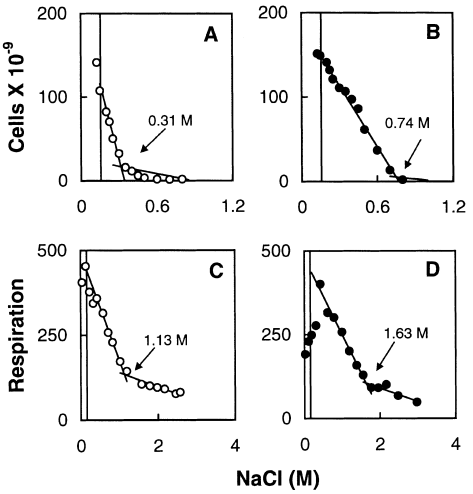

Fig. 8. Effect of glycine betaine on growth and respiration in *E. coli* C90. Growth as cell number and respiration as the specific activity (nanograms of atoms oxygen consumed per minute per milligram of bacterial protein) were plotted as a function of the external NaCl media. Growth was measured as $O.D._{520}$ in the absence [(A), o—o] and presence [(B), ●—●] of 0.5 mM glycine betaine, showing activation volumes of 4324 and 5428 cm^3/mol, respectively. Respiration was measured in the absence [(C), o—o] and presence [(D), ●—●] of 0.5 mM glycine betaine in bacterial cells grown in the presence of 0.3 M NaCl showing activation volumes of 709 and 852 cm^3/mol, respectively.

3.10. The question of leaks vs. growth

Induction of voids in the plasma membrane implies that leak conductance of the membrane is potentially a major variable in the bacterial physiology. Depending on whether one measures a direct permeability related variable such as swelling or a macro event like growth, the mea-

Table 1
Effect of various substrates on the osmoprotective role of glycine betaine on the growth of *E. coli* MC 4100[a]

Substrate	Molecular mass	Critical NaCl, M (break-point)	
		(−) Glycine betaine	(+) Glycine betaine
Glycerol	92	0.39	0.91
Glucose	180	0.35	0.60
Mannitol	182	0.42	0.73
Trehalose	342	0.37	0.40

[a] No relationship was observed with the molecular mass in the presence of glycine betaine (unlike with polyols), when organic acids were used as substrates (data omitted, [28]).

surements reflect variable dependence on the molecular mass of the external osmolyte/substrate. The traditional view is that the bilayer offers a barrier to facilitate the protonmotive force across the bilayer as the energy intermediate for bacterial cells [49]. Thus, bacterial growth and enhanced leak conductance would be inimical to each other. Yet molecular mass dependence (of the substrate) for bacterial growth has been documented and explained in the published literature [50]. The passive permeability of cells to sugars is known to be very low. However, if the passive component of permeability during active transport is considerable (a distinction thus far never been made experimentally), this should directly reflect in growth curves.

Fig. 9 shows a re-examination of the published work on the kinetics of the bacterial growth [8]. It is well known that bacterial growth does not rigorously follow the Michaelis–Menten kinetics [9]. The major methodological problem is the difficulty in measuring the free substrate at low levels during a growth curve reliably. Instances wherein such data were obtained by careful HPLC analyses, it was shown to fit well to a logarithmic model of the kind:

$$\mu = K \cdot \ln(\bar{s}) + a \tag{9}$$

where, μ is the specific growth rate per hour, $\bar{s}$ the growth-limiting substrate concentration, and K and a are appropriate constants. The logarithmic dependence was interpreted to mean a thermodynamic control of growth, J_g, since

$$J_g = \mu = L \cdot \Delta G = L \cdot \{\Delta G^o + RT \cdot \ln([\text{substrate}]/[\text{product}])\} \tag{10}$$

where, ΔG is the Gibbs free-energy difference of the reactions, ΔG^o the standard free-energy difference, L a phenomenological constant of the ensemble of relevant activities, R the gas constant, and T absolute temperature. Table 2 shows an alternative model of leak conductance, i.e.

$$\mu = [\mu_{max} \cdot \bar{s}/(K_s + \bar{s})] + k' \cdot \bar{s} \tag{11}$$

where, μ_{max} is the maximal growth constant and k' the rate constant of the non-saturable leak. The leak would be defined as a non-saturable sink and could be evaluated experimentally by a fit as seen in Fig. 9. The distinction between both models resides not merely on the goodness of fit in terms of the coefficient of correlation obtained by linear least square regression, but a far more rigorous non-parametric criterion that their residuals must be truly random, i.e. without a pattern [8]. The leak model has excellent antecedents, say for anion transport, in erythrocytes [51] and serves

Table 2
The theoretical fits of different models to the bacterial growth in *E. coli* ML30[a]

Models	K_s	V_{max}	Constant	NRSS
(A) Michaelis–Menten model				
1. Hanes–Woolf	0.439	0.869		0.1631
2. Lineweaver–Burk	0.162	0.726		0.1247
3. Eadie–Hofstee	0.157	0.739		0.1175
4. Cornish Bowden	0.290	0.799		0.1070
(B) Logarithmic model			0.290 (K)	0.0472
(C) Leak model	0.134	0.649	0.028 (k')	0.0427

[a] *Notes*. Michaelis–Menten model, $\mu = \mu_{max}[\bar{s}/(k_s + \bar{s})]$; logarithmic model, $\mu = K \cdot \log\bar{s}$; and leak model, $\mu = [\mu_{max} \cdot \bar{s}(k_s + \bar{s})] + k' \cdot \bar{s}$, where μ is the growth rate, μ_{max} maximal growth rate, $\bar{s}$ the substrate concentration, k_s the Michaelis–Menten constant in micromoles, K the rate constant for the logarithmic model, and k' the rate constant of the non-saturable leak [51]. NRSS, the Normalised residual sum of squares is given as: $\text{NRSS} = \sum_i^n (Y_i - \hat{Y})^2 / \sum_i^n (Y_i - \overline{Y})^2$, where, n is the number of observations, Y_i is the observed value, $\hat{Y}$, is the theoretical value, and $\overline{Y}$ is the mean of the observed values.

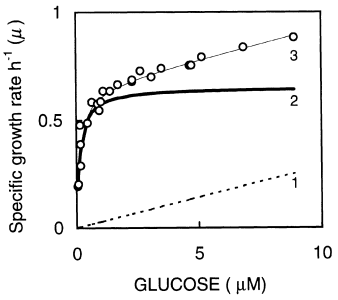

Fig. 9. Growth kinetics data of *E. coli* ML30 fitted to a leak model. Line 1, (...) represents the non-saturable leak component and line 2, (—) the saturable component. Line 3, (o—o) is the leak model as a sum of 2 and 1 (details are given in Section 3.10). Published data was digitised at a precision better than 1% and has been analysed as described in the text.

to bring forth a valuable lesson that there is a need to use rigorous statistical criteria, other than the usual parametric goodness of fit tests in testing models. Variable conductance of bacterial membranes is further supported by the presence of stretch-sensitive channels in the plasma membrane [52,53]. Leak conductance differs in one fundamental way from other conductances in that it reflects a variable that is induced under conditions of active transport and would be absent in the absence of active transport conditions. Since different substrates with independent transporters offer different osmotic sensitivity, it follows that the free energy dissipator (the transporter) has an intimate role in the induction of voids in the lipidic phase.

These results should not be considered irreconcilable with known mechanisms of transport, etc., and offer additional detail on membrane perturbations that osmotic pressure alone cannot reveal. For instance, any uncoupler being also a lipophilic anion, one must distinguish between this aspect of an uncoupler and its presumptive uncoupling action. By definition, an uncoupler should stimulate respiration while it inhibits ATP synthesis or transport. Indeed lactose transport is inhibited by uncouplers as well as respiration under aerobic conditions [31]. Even in the case of cytochrome oxidase vesicles, wherein proton pump activity was measured, the effect of an uncoupler could be seen with the soluble enzyme [54]. This indicates direct effect rather than its uncoupling activity.

In summing up, one should review the special advantage offered by the current osmotic methodology in understanding routine bacterial physiology and energetics, for the directness and insights it offers. For example, maintenance energy could be considered as insensitive or even enhancing with osmotic pressure [55]. This system of coupled equations each one with its own osmotic sensitivity, can also be rewritten for other processes, e.g.

$$J_{A(max)} - \tilde{K}_a \Pi = J_{B(max)} - \tilde{K}_b \Pi + J_{C(max)} - \tilde{K}_c \Pi \quad (12)$$

where, $J_{A(max)}$, $J_{B(max)}$ and $J_{C(max)}$ are the maximal activity or flux of the processes A, B and C respectively, and $\tilde{K}$ is the constant (slope) coupling activity with osmotic pressure, with the lowercase subscript corresponding to respective processes.

Therefore,

$$J_{A(max)} = J_{B(max)} + J_{C(max)} \quad (13)$$

and,

$$\tilde{K}_a \Pi = \tilde{K}_b \Pi + \tilde{K}_c \Pi \quad (14)$$

Thus, in coupled respiration, determining the compressibility coefficients for the induced and endogenous respiration would yield the hidden variable, $\tilde{K}_b \Pi$, or the specifically measured osmotic compressibility of the induced respiration. The present study argues in favour of the intermolecular spaces or voids as causal for this osmotic compressibility.

Though it was argued that water activity itself has less of a role to play than the osmotic pressure on the inhibitory nature of high external solute concentration [48,56,57], and the site of action (inhibition) is the plasma membrane, it was only speculative on the nature of inhibition — conformational change in lipids and/or proteins

of membranes. We conclude, based on the above experimental data, that the change in size distribution of voids (spaces or cavities) in the membrane is responsible for inhibition of membrane-dependent processes and growth. Secondly, we conclude that voids (and hence the leak conductance) have a positive role in the growth and energetics of bacteria.

4. Nomenclature

ANS: 1-Anilinonaphthalene-8-sulfonate
n-AS: *n*-(9-Anthroyloxy) stearic acid
β-Galactosidase: β-D-Galactoside galactohydrolase, EC 3.2.1.23
Catalase hydrogen peroxide: Hydrogen peroxide oxidoreductase, EC 1.11.1.6
DMF: Dimethyl formamide
DMPC: Dimyristoyl phosphatidylcholine
DPH: 1,6-Diphenyl-1,3,5-hexatriene
IPTG: Isopropyl-β-D-thiogalactopyranoside
LUVs: Large unilamellar vesicles
MLVs: Multilamellar vesicles
NRSS: Normalised residual sum of squares
ONPG: *o*-Nitrophenyl-β-D-galactopyranoside
SUV: Small unilamellar vesicles

Acknowledgements

The work was supported by grants to VS from the Department of Science and Technology and the Council of Scientific and Industrial Research. Financial assistance was from the Department of Biotechnology to SN and University Grants Commission, Government of India, to CNM. We thank Dr N.M. Rao and Dr S.B. Kulkarni for their participation during the early phase of this work. We also thank Dr A.D. Gangal for theoretical considerations, Dr M. Patole for critical reading of the MS and constructive suggestions, and Dr G. Krishnamoorthy for help in fluorescence lifetime measurements.

References

[1] K. Rajagopal, V. Sitaramam, Biology of the inner space: voids in biopolymers, J. Theor. Biol. 195 (1998) 245–271.
[2] J.C. Mathai, Z.E. Sauna, O. John, V. Sitaramam, Rate-limiting step in electron transport: osmotically sensitive diffusion of quinones through voids in the bilayer, J. Biol. Chem. 268 (1993) 15442–15454.
[3] R.-S. Pan, Z.E. Sauna, R.A. Dilley, V. Sitaramam, Influence of osmolality of the medium on photosynthetic electron transport, proton fluxes and photophosphorylation in isolated thylakoids, Ind. J. Biochem. Biophys. 32 (1995) 1–10.
[4] S.M. Kaminsky, F.M. Richards, Reduction of thioredoxin significantly decreases its partial specific volume and adiabatic compressibility, Protein Sci. 1 (1992) 22–30.
[5] A. Priev, A. Almagor, S. Yedgar, B. Gavish, Glycerol decreases the volume and compressibility of protein interior, Biochemistry 35 (1996) 2061–2066.
[6] J.-P. Kocher, M. Prevost, S.J. Wodak, B. Lee, Properties of the protein matrix revealed by the free energy of cavity formation, Structure 4 (1996) 1517–1529.
[7] J.C. Mathai, V. Sitaramam, Stretch sensitivity of transmembrane mobility of hydrogen peroxide through voids in the bilayer: role of cardiolipin, J. Biol. Chem. 269 (1994) 17784–17793.
[8] M. Rutgers, M. TeixeiraDe, P.W. Postma, K. vanDam, Establishment of the steady state in glucose-limited chemostat cultures of *Klebsiella pneumoniae*, J. Gen. Microbiol. 133 (1987) 445–453.
[9] M. Rutgers, Control and Thermodynamics of Microbial Growth. Ph.D. Thesis. University of Amsterdam, The Netherlands, 1990.
[10] E.P. Kennedy, Osmotic regulation and the biosynthesis of membrane derived oligosaccharides in *Escherichia coli*, Proc. Natl. Acad. Sci. U. S. A. 79 (1982) 1092–1096.
[11] S.B. Kulkarni, V. Somlata, V. Sitaramam, Assessment of molecular sieving across bacterial outer membrane of *Pseudomonas*, Biochim. Biophys. Acta 1281 (1996) 189–204.
[12] D. Sambasivarao, R. Kramer, N.M. Rao, V. Sitaramam, ATP hydrolysis induces variable porosity to mannitol in the mitochondrial inner membrane, Biochim. Biophys. Acta 933 (1988) 200–211.
[13] A.D. Beavis, A.L. Lehninger, Determination of the upper and lower limits of the mechanistic stoichiometry of incompletely coupled fluxes, Eur. J. Biochem. 158 (1986) 307–314.
[14] O.H. Lowry, N.J. Rosenbrough, A.L. Farr, R.J. Randall, Protein measurement with the folin phenol reagent, J. Biol. Chem. 193 (1951) 265–275.
[15] J.H. Miller, Experiments in Molecular Genetics, Cold Spring Harbour Laboratory, Cold Spring Harbour, New York, 1972.
[16] A.A. Frimer, A. Forman, D.C. Borg, H_2O_2-diffusion through liposomes, Isr. J. Chem. 23 (1983) 442–445.

[17] A.C. Mehly, B. Chance, in: D. Glick (Ed.), Methods in Biochemical Analysis, the Assays of Catalases and Peroxidases, vol. 1, Interscience Publication, New York, 1954, pp. 357–424.
[18] L.A. DelRio, M.G. Ortega, A.L. Lopez, J.L. Gorge, A more sensitive modification of the catalase assay with the Clark oxygen electrode. Application to the kinetic study of the pea leaf enzyme, Anal. Biochem. 80 (1977) 409–415.
[19] F. Szoka Jr., D. Papahadjopoulos, Comparative properties and methods of preparation of lipid vesicles (liposomes), Ann. Rev. Biophys. Bioeng. 9 (1980) 467–508.
[20] M. Shinitzky, Y. Barenholz, Fluidity parameters of lipid regions determined by fluorescence polarization, Biochim. Biophys. Acta 515 (1978) 367–394.
[21] A. Shanubhogue, M.B. Rajarshi, A.P. Gore, V. Sitaramam, Statistical testing of equality of break-points in experimental data, J. Biochim. Biophys. Methods 25 (1992) 95–112.
[22] P.L.-G. Chong, P.A.G. Fortes, D.M. Jameson, Mechanisms of inhibition of (Na^+,K^+)-ATPase by hydrostatic pressure studied with fluorescence probes, J. Biol. Chem. 260 (1985) 14484–14490.
[23] J.B. Stock, B. Rauch, S. Roseman, Periplasmic space in *Salmonella typhimurium* and *Escherichia coli*, J. Biol. Chem. 252 (1977) 7850–7861.
[24] D. Sambasivarao, V. Sitaramam, Respiration induces variable porosity to polyols in the mitochondrial inner membrane, Biochim. Biophys. Acta 806 (1985) 195–209.
[25] A. Nicolli, V. Petronilli, P. Bernardi, Modulation of the mitochondiral cyclosporin A-sensitive permeability transition pore by matrix pH. Evidence that the pore open-closed probability is regulated by reversible histidine protonation, Biochemistry 32 (1993) 4461–4465.
[26] E.K. Hoffman, in: A. Kleinzeller (Ed.), Current Topics in Membranes and Transport, Volume Regulation in Cultured Cells, vol. 30, Academic Press, San Diego, 1987, pp. 125–180.
[27] J.A. Garcia-Horsman, B. Barquera, J. Rumbley, J. Ma, R.B. Gennis, The superfamily of heme-copper respiratory oxidases, J. Bacteriol. 176 (1994) 5587–5600.
[28] N.M. Rao, Studies on Physical Parameters that Influence Membrane Function: Osmotic Pressure as a Physical Probe. Ph.D. thesis. Osmania University, Hyderabad, India, 1987.
[29] E. Pavlasova, F.M. Harold, Energy coupling in the transport of β-galactosides by *Escherichia coli*: effect of proton conductors, J. Bacteriol. 98 (1969) 681–688.
[30] M.A. Williams, J.M. Goodfellow, J.M. Thornton, Buried waters and internal cavities in monomeric proteins, Protein. Sci. 3 (1994) 1224–1235.
[31] H.H. Winkler, T.H. Wilson, The role of energy coupling in the transport of β-galactosides by *Escherichia coli*, J. Biol. Chem. 241 (1966) 2200–2211.
[32] J.C. Mathai, V. Sitaramam, Variable porosity of the mitochondrial inner membrane induced by energization, Biochim. Biophys. Acta 976 (1989) 214–221.
[33] H.J. Hinz, J.M. Sturtevant, Calorimetric studies of dilute aqueous suspensions of bilayers formed from synthetic L-α-lecithins, J. Biol. Chem. 247 (1972) 6071–6075.
[34] R.B. Lentz, Y. Barenholz, T.E. Thompson, Fluorescence depolarization studies of phase transition and fluidity in phospholipid bilayers. 2. Two component phosphatidylcholine liposomes, Biochemistry 15 (1976) 4521–4528.
[35] A. Azzi, B. Chance, G.K. Radda, C.P. Lee, A fluorescence probe of energy-dependent structure changes in fragmented membranes, Biochemistry 62 (1969) 612–619.
[36] P.L. Chong, G. Weber, Pressure dependence of 1,6-diphenyl-1,3,5-hexatriene fluorescence in single component phosphatidylcholine liposomes, Biochemistry 22 (1983) 5544–5550.
[37] A.G. Lee, Functional properties of biological membranes: a physical chemical approach, Prog. Biophys. Mol. Biol. 29 (1975) 3–56.
[38] F.J. Nagle, Theory of the main lipid bilayer phase transition, Ann. Rev. Phys. Chem. 31 (1980) 157–195.
[39] H.J. Trauble, The movement of molecules across lipid membranes: a molecular theory, J. Membr. Biol. 4 (1971) 193–208.
[40] C. Ho, S.J. Slater, C.D. Stubbs, Hydration and order in lipid bilayers, Biochemistry 34 (1995) 6188–6195.
[41] B. Withoult, M. Boekhout, M. Brock, J. Kingma, H.V. Heerikhuizen, L.D. Leij, An efficient and reproducible procedure for the formation of spheroplasts from variously grown *Escherichia coli*, Anal. Biochem. 74 (1976) 160–170.
[42] L.N. Csonka, A.D. Hanson, Prokaryotic osmoregulation: genetics and physiology, Annu. Rev. Microbiol. 45 (1991) 569–606.
[43] S. Cayley, B.A. Lewis, H.J. Guttman, M.T. Record, Jr., Characterization of the cytoplasm of *Escherichia coli* K-12 as a function of external osmolarity: implications for protein–DNA interactions in vivo, J. Mol. Biol. 222 (1991) 281–300.
[44] S. Cayley, B.A. Lewis, T.M. Record, Jr., Origins of the osmoprotective properties of betaine and proline in *Escherichia coli* K-12, J. Bacteriol. 174 (1992) 1586–1595.
[45] B. Perroud, D. Le Rudulier, Glycine betaine transport in *Escherichia coli*: osmotic modulation, J. Bacteriol. 161 (1985) 393–401.
[46] J. Boch, B. Kempf, E. Bremer, Osmoregulation in *Bacillus subtilis*: synthesis of the osmoprotection glycine betaine from exogenously provided choline, J. Bacteriol. 176 (1994) 5364–5371.
[47] S. Mikkat, M. Hagemann, A. Schoor, Active transport of glucosylglycerol is involved in salt adaptation of the cyanobacterium *Synechocystis* sp. strain PCC 6803, Microbiology 142 (1996) 1725–1732.
[48] R.P. Walter, G.J. Morris, D.B. Kell, The roles of osmotic stress and water activity in the inhibition of the growth, glycolysis and glucose phosphotransferase system of *Clostridium pasteurianum*, J. Gen. Microbiol. 133 (1987) 259–266.

[49] P.C. Maloney, *Escherichia coli* and *Salmonella typhimurium*: cellular and molecular biology, in: F.C. Neidhardt (Ed.), Coupling to an Energized Membrane: Role of Ion-motive Gradients in the Transduction of Metabolic Energy, vol. 1, American Society for Microbiology, Washington, 1987, pp. 222–243.

[50] H. Nikaido, E.Y. Rosenberg, Effect of solute size on diffusion rates through the transmembrane pores of the outer membrane of *Escherichia coli*, J. Gen. Physiol. 77 (1981) 121–135.

[51] D. Colquhoun, R. Henderson, J.M. Ritchie, The binding of labelled tetradotoxin to non-myelinated nerve fibres, J. Gen. Physiol. 227 (1973) 95–126.

[52] S.I. Sukharev, B. Martinac, V.Y. Arshavsky, C. Kung, Cooperative mechanosensitive ion channels in *Escherichia coli*, Biophys. J. 65 (1993) 177–183.

[53] C. Cui, D.O. Smith, J. Adler, Characterization of mechanosensitive channels in *Escherichia coli* cytoplasmic membrane by whole-cell patch recording, J. Membr. Biol. 144 (1995) 31–42.

[54] V. Sitaramam, D. Sambasivarao, J.C. Mathai, Differential effects of osmotic pressure on mitochondrial respiratory chain and indices of oxidative phosphorylation, Biochim. Biophys. Acta 975 (1989) 252–266.

[55] V. Sitaramam, C.N. Madhavarao, The energetic basis of osmotolerance in plants: physical principles, J. Theor. Biol. 189 (1997) 333–352.

[56] A.G. Macdonald, The effects of pressure on the molecular structure and physiological functions of cell membranes, Philos. Trans. R. Soc. B 304 (1984) 47–68.

[57] W.G. Roth, S.E. Porter, M.P. Leckie, B.E. Porter, D.N. Dietzler, Restoration of cell volume and the reversal of carbohydrate transport and growth of osmotically upshocked *Escherichia coli*, Biochem. Biophys. Res. Commun. 126 (1985) 442–449.